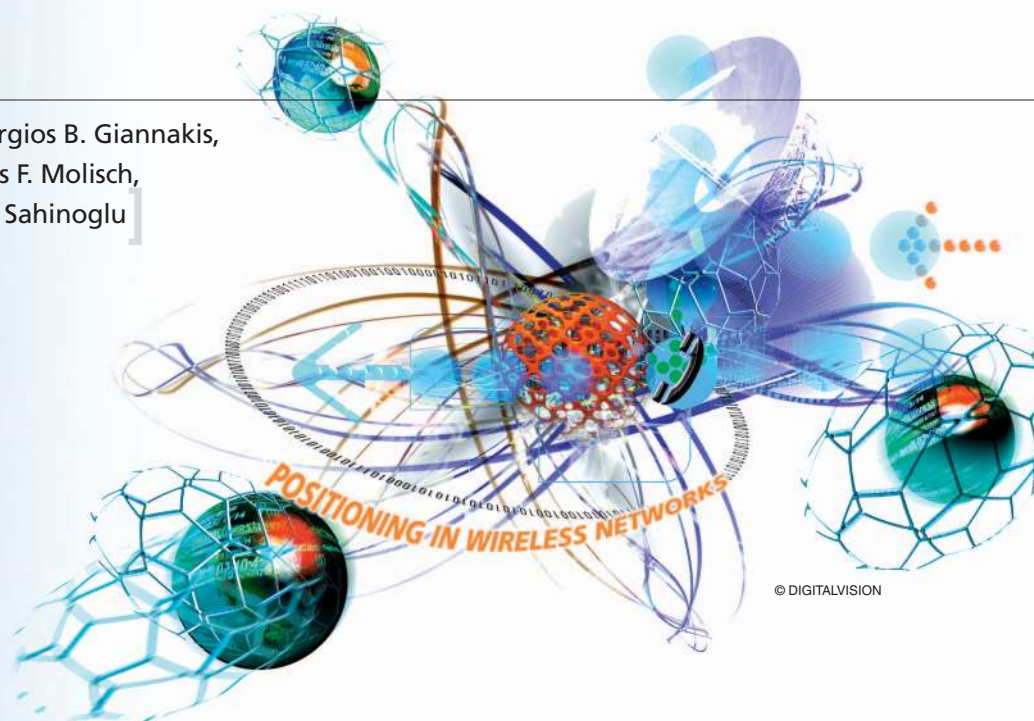Sinan Gezici, Zhi Tian, Georgios B. Giannakis,
Hisashi Kobayashi, Andreas F. Molisch,
H. Vincent Poor, and Zafer Sahinoglu

Localization via Ultra-Wideband Radios

[A look at positioning aspects of future sensor networks]

Ultra-wideband (UWB) radios have relative bandwidths larger than 20% or absolute bandwidths of more than 500 MHz. Such wide bandwidths offer a wealth of advantages for both communications and radar applications. In both cases, a large bandwidth improves reliability, as the signal contains different frequency components, which increases the probability that at least some of them can go through or around obstacles. Furthermore, a large absolute bandwidth offers high resolution radars with improved ranging accuracy. For communications, both large relative and large absolute bandwidth alleviate small-scale fading [1], [2]; furthermore, spreading information over a very large bandwidth decreases the power spectral density, thus reducing interference to other systems, effecting spectrum overlay with legacy radio services, and lowering the probability of interception.

UWB radars have been of long-standing interest, as they have been used in military applications for several decades [3], [4]. UWB communications-related applications were introduced only in the early 1990s [5]–[7], but have received wide interest after the U.S. Federal Communications Commission (FCC) allowed the use of *unlicensed* UWB communications [8]. The first commercial systems, developed in the context of the IEEE 802.15.3a standardization process, are intended for high data rate, short range personal area networks (PANs) [9]–[11].

Emerging applications of UWB are foreseen for sensor networks as well. Such networks combine low to medium rate communications with positioning capabilities. UWB signaling is especially suitable in this context because it allows centimeter accuracy in ranging, as well as

low-power and low-cost implementation of communication systems. These features allow a new range of applications, including logistics (package tracking), security applications (localizing authorized persons in high-security areas), medical applications (monitoring of patients), family communications/supervision of children, search and rescue (communications with fire fighters, or avalanche/earthquake victims), control of home appliances, and military applications.

These new possibilities have also been recognized by the IEEE, which has set up a new standardization group 802.15.4a for the creation of a new physical layer for low data rate communications combined with positioning capabilities; UWB technology is a leading candidate for this standard.

While UWB positioning bears similarities to radar, there are distinct differences. For example, radar typically relies on a stand-alone transmitter/receiver, whereas a sensor network combines information from multiple sensor nodes to refine the position estimate. On the other hand, a radar can usually choose a location where surroundings induce minimal clutter, while a sensor node in a typical application cannot choose its location and must deal with nonideal or even harsh electromagnetic propagation conditions. Finally, sensor networks operate in the presence of multiple-access interference, while radar is typically influenced more by narrowband interferers (jammers).

UWB communication has been discussed recently in [12]–[15]. In this article, we concentrate on positioning aspects of future sensor networks. Positioning systems can be divided into three main categories: time-of-arrival, direction-of-arrival, and signal-strength based systems. We will discuss their individual properties, including fundamental performance bounds in the presence of noise and multipath. Furthermore, we will describe possible combination strategies that improve the overall performance.

In this special section of *IEEE Signal Processing Magazine*, various aspects of signal processing techniques for positioning and navigation with applications to communication systems are covered. For example, in [16], a number of positioning techniques are investigated from a system's point of view for cellular networks, wireless local area networks (LANs) and ad-hoc sensor networks. The positioning problem for cellular networks is further discussed in [17], which considers theoretical bounds and the FCC's requirements on locating emergency calls. The treatment in that work spans dynamic and static models for positioning given a set of measurements; it does not, however, consider low-layer issues such as specific timing estimation algorithms. These low-layer issues, such as time of arrival and angle of arrival estimation algorithms, are studied in [18]. Positioning in wireless sensor networks is further investigated in [19], which focuses on cooperative (multihop) localization. Among the possible signal-

ing schemes discussed in [19], UWB signaling is presented as a good candidate for short-range accurate location estimation. Our purpose is to investigate the positioning problem from a UWB perspective and to present performance bounds and estimation algorithms for UWB ranging/positioning.

POSITIONING TECHNIQUES FOR UWB SYSTEMS

Locating a node in a wireless system involves the collection of location information from radio signals traveling between the target node and a number of reference nodes. Depending on the positioning technique, the angle of arrival (AOA), the signal strength (SS), or time delay information can be used to determine the location of a node [20]. The AOA technique measures the angles between a given node and a number of reference nodes to estimate the location, while the SS and time-based approaches estimate the distance between nodes by measuring the energy and the travel time of the received signal, respectively. We will investigate each approach from the viewpoint of a UWB system.

AOA

An AOA-based positioning technique involves measuring angles of the target node seen by reference nodes, which is done by means of antenna arrays. To determine the location of a node in a two-dimensional (2-D) space, it is sufficient to measure the angles of the straight lines that connect the node and two reference nodes, as shown in Figure 1.

The AOA approach is not suited to UWB positioning for the following reasons. First, use of antenna arrays increases the system cost, annulling the main advantage of a UWB radio equipped with low-cost transceivers. More importantly, due to the large bandwidth of a UWB signal, the number of paths may be very large, especially in indoor environments. Therefore, accurate angle estimation becomes very challenging due to scattering from objects in the environment. Moreover, as we will see later, time-based approaches can provide very precise location estimates, and therefore they are better motivated for UWB over the more costly AOA-based techniques.

SS

Relying on a path-loss model, the distance between two nodes can be calculated by measuring the energy of the
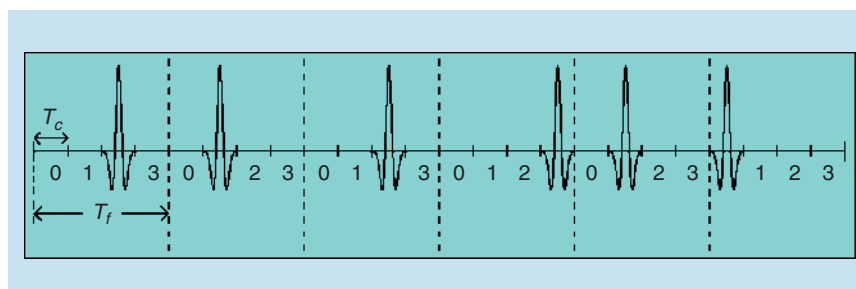
[FIG1] A sample transmitted signal from a time-hopping impulse radio UWB system. T_f is the frame time and T_c is the chip interval. The locations of the pulses in the frames are determined according to a time-hopping sequence. See [6] for details.

received signal at one node. This distance-based technique requires at least three reference nodes to determine the 2-D location of a given node, using the well-known triangulation approach depicted in Figure 2 [20]. To determine the distance from SS measurements, the characteristics of the channel must be known. Therefore, SS-based positioning algorithms are very sensitive to the estimation of those parameters.

The Cramér-Rao lower bound (CRLB) for a distance estimate $\hat{d}$ from SS measurements provides the following inequality [21]:

$$\sqrt{\text{Var}(\hat{d})} \geq \frac{\ln 10}{10} \frac{\sigma_{sh}}{n_p} d, \qquad (1)$$

where d is the distance between the two nodes, n_p is the path loss factor, and σ_{sh} is the standard deviation of the zero mean Gaussian random variable representing the log-normal channel shadowing effect. From (1), we observe that the best achievable limit depends on the channel parameters and the distance between the two nodes. Therefore, the unique characteristic of a UWB signal, namely the very large bandwidth, is not exploited to increase the best achievable accuracy. In some cases, however, the target node can be very close to some reference nodes, such as relay nodes in a sensor network, which can take SS measurements only [22]. In such cases, SS measurements can be used in conjunction with time delay measurements of other reference nodes in a hybrid scheme, which can help improve the location estimation accuracy. The fundamental limits for such a hybrid scheme are investigated later.

TIME-BASED APPROACHES
Time-based positioning techniques rely on measurements of travel times of signals between nodes. If two nodes have a common clock, the node receiving the signal can determine the time of arrival (TOA) of the incoming signal that is time-stamped by the reference node. For a single-path

[FIG2] Positioning via the AOA measurement. The blue (dark) nodes are the reference nodes.

additive white Gaussian noise (AWGN) channel, it can be shown that the best achievable accuracy of a distance estimate $\hat{d}$ derived from TOA estimation satisfies the following inequality [23], [24]:

$$\sqrt{\text{Var}(\hat{d})} \geq \frac{c}{2\sqrt{2}\pi \sqrt{\text{SNR}} \beta}, \qquad (2)$$

where c is the speed of light, SNR is the signal-to-noise ratio, and β is the effective (or root mean square) signal bandwidth defined by

$$\beta \triangleq \left[\int_{-\infty}^{\infty} f^2 |S(f)|^2 df \Big/ \int_{-\infty}^{\infty} |S(f)|^2 df \right]^{1/2}, \qquad (3)$$

and $S(f)$ is the Fourier transform of the transmitted signal.

Unlike SS-based techniques, the accuracy of a time-based approach can be improved by increasing the SNR or the effective signal bandwidth. Since UWB signals have very large bandwidths, this property allows extremely accurate location estimates using time-based techniques via UWB radios. For example, with a receive UWB pulse of 1.5 GHz bandwidth, an accuracy of less than an inch can be obtained at SNR = 0 dB.

Since the achievable accuracy under ideal conditions is very high, clock synchronization between the nodes becomes an important factor affecting TOA estimation accuracy. Hence, clock jitter must be considered in evaluating the accuracy of a UWB positioning system [25].

If there is no synchronization between a given node and the reference nodes, but there is synchronization among the reference nodes, then the time-difference-of-arrival (TDOA) technique can be employed [20]. In this case, the TDOA of two signals traveling between the given node and two reference nodes is estimated, which determines the location of the node on a hyperbola, with foci at the two reference nodes. Again a third reference node is needed for localization. In the absence of a common clock between the nodes, round-trip time between two transceiver nodes can be measured to estimate the distance between two nodes [26], [27].

In a nutshell, for positioning systems employing UWB radios, time-based schemes provide very good accuracy due to the high time resolution (large bandwidth) of UWB signals. Moreover, they are less costly than the AOA-based schemes, the latter of which is less effective for typical UWB signals experiencing strong scattering. Although it is easier to estimate SS than TOA, the range information obtained from SS measurements is very coarse compared to that obtained from the TOA measurements. Due to the inherent suitability and accuracy of time-based approaches for UWB systems, we will focus our discussion on time-based UWB positioning in the rest of this article, except for the SS-TOA hybrid algorithm.
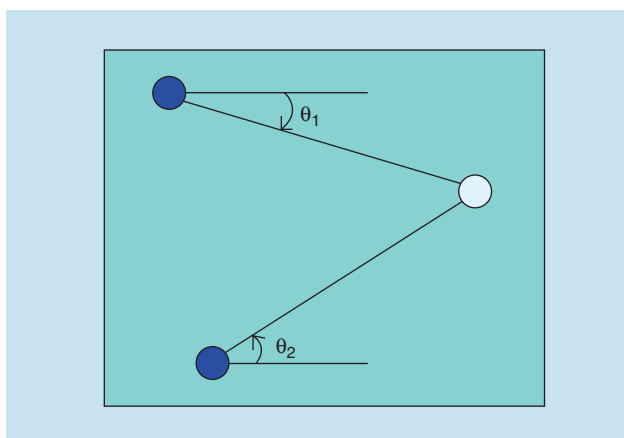
TIME-BASED UWB POSITIONING AND MAIN SOURCES OF ERROR

Detection and estimation problems associated with a signal traveling between nodes have been well studied in radar and other applications. An optimal estimate of the arrival time is obtained using a matched filter, or equivalently, a bank of correlation receivers (see [28]). In the former approach the instant at which the filter output attains its peak provides the arrival time estimate, whereas in the latter, the time shift of the template signal that yields the largest cross correlation with the received signal gives the desired estimate. These two estimates are mathematically equivalent, so the choice is typically based on design and implementation costs. The correlation receiver approach requires a possibly large number of correlators in parallel (or computations of cross correlation in parallel). Alternatively, the matched filter approach requires only a single filter, but its impulse response must closely approximate the time-reversed version of the received signal waveform plus a device or a program that can identify the instant at which the filter output reaches its peak.

The maximum likelihood estimate (MLE) of the arrival time can be also reduced to the estimate based on the matched filter or correlation receiver, when the communication channel can be modeled as an AWGN channel (see also [28]). It is also well known in radar theory (see, e.g., [24]) that this MLE achieves the CRLB asymptotically. It can be shown, for AWGN channels, that a set of TOAs determined from the matched filter outputs is a sufficient statistic for obtaining the MLE or maximum a posteriori (MAP) probability estimate of the location of the node in question (see [29]–[32]).

Instead of the optimal MLE/MAP location estimate, the conventional TOA-based scheme estimates the location of the node using the lower-complexity least squares (LS) approach [20]:

$$\hat{\boldsymbol{\theta}} = \arg\min_{\boldsymbol{\theta}} \sum_{i=1}^{N} w_i \left[\tau_i - d_i(\boldsymbol{\theta})/c \right]^2, \qquad (4)$$

where N is the number of reference nodes, τ_i is the ith TOA measurement, $d_i(\boldsymbol{\theta}) := \|\boldsymbol{\theta} - \boldsymbol{\theta}_i\|$ is the distance between the given node and the ith reference node, with $\boldsymbol{\theta}$ and $\boldsymbol{\theta}_i$ denoting their locations respectively, and w_i is a scalar weighting factor for the ith measurement that reflects the reliability of the ith TOA estimate.

Although location estimation can be performed in a straightforward manner using the conventional LS technique represented by (4) for a single user, line-of-sight (LOS) and single-path environment, it becomes challenging when more realistic situations are considered. In such scenarios, the main sources of errors are multipath propagation, multiple access interference (MAI), and non-line-of-sight (NLOS) propagation. In addition, for UWB systems in particular, realizing the purported high location resolution faces major challenges in accurate timing of ultrashort pulses of ultralow power density.

MULTIPATH PROPAGATION

In conventional matched filtering or correlation-based TOA estimation algorithms, the time at which the matched filter output peaks, or, the time shift of the template signal that produces the maximum correlation with the received signal is used as the TOA estimate. In a narrowband system, however, this value may not be the true TOA since multiple replicas of the transmitted signal, due to multipath propagation, partially overlap and shift the position of the correlation peak. In other words, the multipath channel creates mismatch between the received signal of interest and the transmitted template used; as a result, instead of auto-correlation, we obtain a cross-correlation, which does not necessarily peak at the correct timing. To prevent this effect, some high resolution time delay estimation techniques, such as that described in [33], have been proposed. These techniques are very complex compared to the correlation based algorithms. Fortunately, due to the large bandwidth of a UWB signal, multipath components are usually resolvable without the use of complex algorithms. However, multiple correlation peaks are still present and it is important to consider algorithms such as that proposed in [26] to detect the first arriving signal path; see also [34]–[38] for improved recent alternatives.

## MULTIPLE ACCESS INTERFERENCE

In a multiuser environment, signals from other nodes interfere with the signal of a given node and degrade performance of time delay estimation.

A technique for reducing the effects of MAI is to use different time slots for transmissions from different nodes. For example, in the IEEE 802.15.3 PAN standard [39], transmissions from different nodes are time division multiplexed so that no two nodes in a given piconet transmit at the same time. However, even with such time multiplexing, there can still be MAI from neighboring piconets and MAI is still an issue. Furthermore, time multiplexing is often undesirable since spectral efficiency can be reduced by channelization.

NLOS PROPAGATION

When the direct LOS between two nodes is blocked, only reflections of the UWB pulse from scatterers reach the receiving node. Therefore, the delay of the first arriving pulse does not represent the true TOA. Since the pulse travels an extra distance, a positive bias called the NLOS error is present in the measured time delay. In this case, using the LS technique in (4) causes large errors in the location estimation process, since the LS solution is MLE optimal only when each measurement error is a zero mean Gaussian random variable with known variance.

In the absence of any information about NLOS errors, accurate location estimation is impossible. In this case, some non-parametric (pattern recognition) techniques, such as those in [40] and [41], can be employed. The main idea behind nonparametric location estimation is to gather a set of TOA measurements from all the reference nodes at *known* locations beforehand and use this set as a reference when a new set of measurements is obtained.
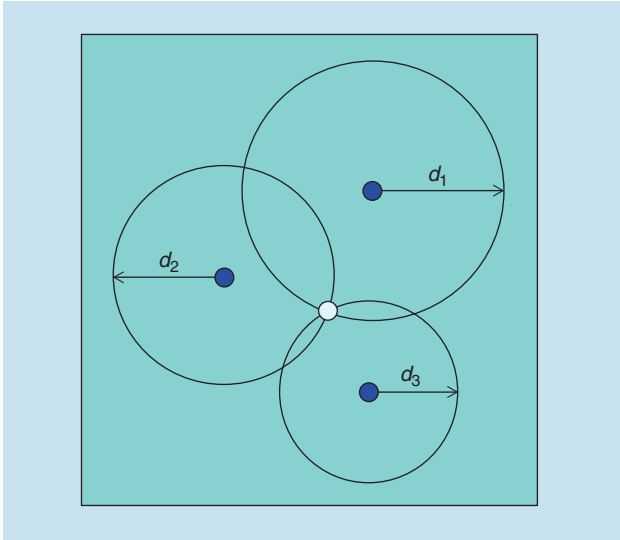
[FIG3] Distance-based positioning technique. The distances can be obtained via the SS or the TOA estimation. The blue (dark) nodes are the reference nodes.

In practical systems, however, it is usually possible to obtain some statistical information about the NLOS error. Wylie and Holtzman [42] observed that the variance of the TOA measurements in the NLOS case is usually much larger than that in the LOS case. They rely on this difference in the variance to identify NLOS situations and then use a simple LOS reconstruction algorithm to reduce the location estimation error. Also, by assuming a scattering model for the environment, the statistics of TOA measurements can be obtained, and then well-known techniques, such as MAP and ML, can be employed to mitigate the effects of NLOS errors [43], [44]. In the case of tracking a mobile user in a wireless system, biased and unbiased Kalman filters can be employed to estimate the location accurately [45], [41].

In addition to introducing a positive bias, NLOS propagation may also cause a situation where the first arriving pulse is usually not the strongest pulse. Therefore, conventional TOA estimation methods that choose the strongest path would introduce another positive bias into the estimated TOA. In UWB positioning systems, first path detection algorithms [26], [46] have been proposed to mitigate the effects of the NLOS error.

Later we will consider a unified analysis of the NLOS location estimation problem and present estimators that are asymptotically optimal in the presence and absence of statistical NLOS information [32].

HIGH TIME RESOLUTION OF UWB SIGNALS
As we have noted above, the extremely large bandwidth of UWB signals results in very high temporal (and thus spatial) resolution. On the other hand, it also imposes challenges to accurate TOA estimation in practical systems.

First, clock jitter becomes an important factor in evaluating the accuracy of UWB positioning systems [25]. Since UWB pulses have very short (subnanosecond) duration, clock accuracies and drifts in the target and the reference nodes affect the TOA estimates.

Another consequence of high time resolution inherent in UWB signals is the uncertainty region for TOA; that is, the set of delay positions that includes TOA is usually very large compared to the chip duration. In other words, a large number of chips need to be searched for TOA. This makes conventional correlation-based serial search approaches impractical, and calls for fast TOA estimation schemes.

Finally, high time resolution, or equivalently large bandwidth, of UWB signals makes it very impractical to sample the received signal at or above the Nyquist rate, which is typically on the order of tens of GHz. To facilitate low-power UWB radio designs, it is essential to perform high-performance TOA estimation at affordable complexity, preferably by making use of frame-rate or symbol-rate samples.

FUNDAMENTAL LIMITS FOR TOA ESTIMATION
In this section, we delineate the fundamental limits of TOA estimation and present means of realizing the high time resolution of UWB signals at affordable complexity. For positioning applications, we focus on TOA estimation for a single link between the target node and a reference node. We start with deriving the CRLB of TOA estimation achieved by the ML estimator [47] for a realistic UWB multipath channel [48], [49].

CRLB FOR TOA ESTIMATION IN MULTIPATH CHANNELS
In a UWB positioning system, a reference node transmits a stream of ultrashort pulses $p(t)$ of duration T_p at the nanosecond scale. Each symbol is conveyed by repeating over N_f frames one pulse per frame (of frame duration $T_f \gg T_p$), resulting in a low duty cycle transmission form [50]. Every frame contains N_c chips, each of chip duration T_c. Once timing is acquired at the receiver's end, node separation can be accomplished with node-specific pseudorandom time-hopping (TH) codes $\{c[i]\} \in [0, N_c - 1]$, which time-shift the pulse positions at multiples of T_c [50], as shown in Figure 3. The symbol waveform comprising N_f frames is given by $p_s(t) := \sum_{i=0}^{N_f-1} p(t - c[i]T_c - iT_f)$, which has symbol duration $T_s := N_f T_f$. The transmitted UWB waveform is given by

$$s(t) = \sqrt{\varepsilon} \sum_{k=-\infty}^{+\infty} a[k]p_s(t - kT_s - b[k]\Delta), \qquad (5)$$

where ε is the transmission energy per symbol and Δ is the modulation index on the order of T_p. With $s[k] \in [0; M - 1]$ denoting the Mary symbol transmitted by the reference node during the kth symbol period. Equation (5) subsumes two commonly used modulation schemes, pulse position modulation (PPM) for which $b[k] = s[k]$, and $a[k] = 1$ for all k and pulse amplitude modulation (PAM) for which $a[k] = s[k]$ and $b[k] = 0$ for all k [50], [51].

Adopting a tapped delay line multipath channel model, the received signal after multipath propagation is

$$r(t) = \sum_{j=1}^{L} \alpha_j s(t - \tau_j) + n(t), \qquad (6)$$

where L is the number of paths, with path amplitudes $\{\alpha_j\}$ and delays $\{\tau_j\}$ satisfying $\tau_j < \tau_{j+1}$, $\forall j$. The noise $n(t)$ is approximated as a zero-mean white Gaussian process with double-sided power spectral density $N_0/2$ [52].

Let us collect the unknown path gains and delays in (6) into a $2L \times 1$ channel parameter vector

$$\boldsymbol{\theta} = [\alpha_1, \ldots, \alpha_L, \tau_1, \ldots, \tau_L]^T. \tag{7}$$

The received signal is observed over an interval $t \in [0, T_0]$, with $T_0 = KT_s$ spanning K symbol periods. The log-likelihood function of $\boldsymbol{\theta}$ takes the form [47]

$$\ln[\Lambda(\boldsymbol{\theta})] = -\frac{1}{N_o} \int_0^{T_0} \left| r(t) - \sum_{j=1}^{L} \alpha_j s(t - \tau_j) \right|^2 dt. \tag{8}$$

Taking the second-order derivative of (8) with respect to $\boldsymbol{\theta}$, we obtain the Fisher information matrix (FIM) after straightforward algebraic manipulations

$$\mathbf{F}_{\boldsymbol{\theta}} = \begin{bmatrix} \mathbf{F}_{\alpha\alpha} & \mathbf{F}_{\alpha\tau} \\ \mathbf{F}_{\alpha\tau} & \mathbf{F}_{\tau\tau} \end{bmatrix}, \tag{9}$$

where $\mathbf{F}_{\alpha\alpha} := (KN_f \mathcal{E}\mathcal{E}_p/\mathcal{N}_o)\mathbf{I}$, $\mathbf{F}_{\alpha\tau} := -(KN_f \mathcal{E}\mathcal{E}_p'/\mathcal{N}_o) \operatorname{diag} \{\alpha_1, \ldots, \alpha_L\}$ and $\mathbf{F}_{\tau\tau} := (KN_f \mathcal{E}\mathcal{E}_p''/\mathcal{N}_o) \operatorname{diag}\{\alpha_1^2, \ldots, \alpha_L^2\}$; $\mathcal{E}_p$, $\mathcal{E}_p'$, and $\mathcal{E}_p''$ are energy-related constants determined by the pulse shape $p(t)$ and its derivative $p'(t) := \partial p(t)/\partial t$; and $\operatorname{diag}\{\cdot\}$ denotes a diagonal matrix. When there is no overlap between neighboring signal paths, it follows that $\mathcal{E}_p := \int_0^{T_p} p^2(t)dt$, $\mathcal{E}_p' := \int_0^{T_p} p(t)p'(t)dt = [p^2(T_p) - p^2(0)]/2$, and $\mathcal{E}_p'' := \int_0^{T_p}[p'(t)]^2 dt$. Based on (9), the CRLB of each time delay estimate $\hat{\tau}_j$, $j = 1, \ldots, L$, is given by

$$\begin{aligned} \text{CRB}(\hat{\tau}_j) &= \left[(\mathbf{F}_{\tau\tau} - \mathbf{F}_{\alpha\tau}\mathbf{F}_{\alpha\alpha}^{-1}\mathbf{F}_{\alpha\tau})^{-1} \right]_{j,j} \\ &= \frac{\mathcal{N}_o}{KN_f \mathcal{E}(\mathcal{E}_p'' - \mathcal{E}_p'^2/\mathcal{E}_p)\alpha_j^2}. \end{aligned} \tag{10}$$

As a special case, when $L = 1$ and $|p(0)| = |p(T_p)|$, (10) reduces to its AWGN counterpart given in [53]

$$\text{CRB}(\hat{\tau}_1) = \frac{\mathcal{N}_o}{KN_f \mathcal{E}\mathcal{E}_p''\alpha_1^2}, \quad \mathcal{E}_p'' = \frac{\int_{-\infty}^{\infty} f^2 |P(f)|^2 df}{\int_{-\infty}^{\infty} |P(f)|^2 df}, \tag{11}$$

where $P(f)$ is the Fourier transform of $p(t)$. Depending on whether $s[k]$ is deterministic or random, for the data-aided versus blind cases, (10) and (11) are exact CRLBs in the data-aided case and represent the looser modified CRB (MCRB) in the non-data-aided case [54]. It is evident from (10) that the

fundamental lower limit to the variance of a UWB timing estimator is determined by the pulse shape $p(t)$, path gains $\{\alpha_j^2\}$, and the observation interval KT_s, which in turn relates to the pulse repetition gain N_f.

Albeit useful in benchmarking performance, the CRLB in (10) is quite difficult to approach when synchronizing a practical UWB receiver. The difficulty is rooted in the unique characteristics of UWB signaling induced by its ultrawide bandwidth. TOA estimation via the ML principle requires sampling at or above the Nyquist rate, which results in a formidable sampling rate of 14.3–35.7 GHz for a typical UWB monocycle of duration 0.7 ns [47]. Such a high sampling rate might be essential in achieving high-performance TOA estimation in AWGN or low-scattering channels. For multipath channels with inherent large diversity, on the other hand, recent research has led to low-complexity TOA estimators that sample at much lower rates of one sample per frame or even per symbol [34]–[38]. Therefore, the CRLB is more pertinent for outdoor applications where low-scattering channels prevail but not necessarily so for strong-scattering channels that characterize dense-multipath indoor environments in emerging commercial applications of UWB radios. In the latter case, computational complexity limits the applicability of ML timing estimators in addition to implementation constraints imposed at the A/D modules. In such indoor environments, a very large number of closely spaced channel taps must be estimated from a very large sample set, to capture sufficient symbol energy from what has been scattered by dense multipath [47], [55]–[57]. Another complication in ML estimation is the pulse distortion issue in UWB propagation [58]. Frequency-dependent pulse distortion results in nonideal receive-templates, which further degrades the performance of ML estimation. There is clearly a need for practical timing estimation methods that properly account for the unique features of UWB transmissions.

Next, we present rapid UWB-based low-complexity TOA estimators that bypass pulse-rate sampling and path-by-path channel parameter estimation. Variance expressions of such timing estimators provide meaningful measures for evaluating the performance of practical UWB positioning systems.

> **POSITIONING SYSTEMS CAN BE DIVIDED INTO THREE MAIN CATEGORIES: TIME-OF-ARRIVAL, DIRECTION-OF-ARRIVAL, AND SIGNAL-STRENGTH BASED SYSTEMS.**

LOW-COMPLEXITY TOA ESTIMATION IN DENSE MULTIPATH

The key idea behind low-complexity TOA estimation is to consider the aggregate unknown channel instead of resolving all closely spaced paths. As we will show, it suffices to estimate only the first path arrival from the LOS nodes to effect asymptotically optimal UWB-based geolocation. Isolating the first arrival time τ_1, other path delays can be uniquely described as $\tau_{j,1} := \tau_j - \tau_1$ with respect to τ_1. It is then convenient to express $r(t)$ in terms of the *aggregate receive-pulse* $p_R(t)$ that encompasses the

transmit-pulse, spreading codes and multipath effects [c.f. (5) and (6) taking PAM as an example]:

$$r(t) = \sqrt{\mathcal{E}} \sum_{k=0}^{\infty} s[k] p_R(t - kT_s - \tau_1) + n(t),$$

$$\text{where} \quad p_R(t) := \sum_{j=1}^{L} \alpha_j p_s(t - \tau_{j,1}). \tag{12}$$

We select $T_f \geq \tau_{L,1} + T_p$ and $c_0 \geq c_{N_f - 1}$ to confine the duration of $p_R(t)$ within $[0, T_s]$ and avoid intersymbol interference (ISI). Timing synchronization amounts to estimating τ_1, which can be accomplished in two stages. First, we use energy detection to estimate $\lfloor \tau_1/T_s \rfloor$, where $\lfloor \cdot \rfloor$ denotes integer floor [35], [38]. This effectively yields a coarse timing offset estimate in terms of integer multiples of the symbol period. Subsequently, we must estimate the residual fine-scale timing offset ($\tau_1 \mod T_s$), which critically affects localization accuracy. To this end, we

henceforth confine τ_1 within a symbol duration; i.e., $\tau_1 \in [0, T_s]$. Traditionally, τ_1 is estimated by peak-picking the correlation of $r(t)$ with the ideal template $p_R(t)$. The challenge here is that no clean template for matching is available, since the multipath channel (and thus $p_R(t)$) is unknown. If, on the other hand, we select the transmit template $p_s(t)$, timing is generally not identifiable because multiple peaks emerge in the correlator output due to the unknown multipath channel.

Our first step is to establish a noisy template that matches the unknown multipath channel. Estimating $p_R(t)$ from $r(t)$ requires knowledge of τ_1, which is not available prior to timing. For this reason, we will obtain instead a mistimed (by τ_1) version of $p_R(t)$, which we will henceforth denote as $p_R(t; \tau_1)$, $t \in [0, T_s]$. With reference to the receiver's clock, $p_R(t; \tau_1)$ is nothing but a T_s-long snapshot of the delayed periodic receive waveform $\tilde{p}_R(t; \tau_1) := \sum_{k=0}^{\infty} p_R(t - kT_s - \tau_1)$ within the time window $[0, T_s]$. It is evident from (12) that the channel components in $\tilde{p}_R(t; \tau_1)$ are in sync with those contained in the received waveform $r(t)$; thus $p_R(t; \tau_1)$ is the ideal template for a symbol-rate correlator to collect all the channel path energy in the absence of timing information [35], [38]. To estimate $p_R(t; \tau_1)$, we suppose that a training sequence of all ones ($s[k] = 1, \forall k$) is observed within an interval of K_1 symbol periods. Within this observation window, the noise-free version of the received signal is nothing but the aggregate channel $p_R(t; \tau_1)$ itself being amplified by $\sqrt{\mathcal{E}}$ and periodically repeated every T_s seconds. We can thus obtain the estimate $\hat{p}_R(t; \tau_1) = (1/K_1) \sum_{k=0}^{K_1-1} r(t + kT_s)$, $t \in [0, T_s]$, which involves analog operations of delay and average over consecutive symbol-long segments of $r(t)$. We periodically extend $\hat{p}_R(t; \tau_1)$ to obtain the waveform $\hat{\tilde{p}}_R(t; \tau_1) = \sum_{k=0}^{\infty} \hat{p}_R(t + kT_s; \tau_1)$ [59], whose noise-free ver-

sion is given by $\sqrt{\mathcal{E}} \tilde{p}_R(t; \tau_1)$. When a correlation receiver is employed, we will use $\hat{\tilde{p}}_R(t; \tau_1)$ as the asymptotically optimal (in K_1) correlation template for matching $r(t)$, thus effecting sufficient energy capture without tap-by-tap channel estimation.

During synchronization, the receiver generates symbol-rate samples at *candidate* time shifts $\tau \in [0, T_s]$:

$$y_k(\tau) = \int_{\tau + kT_s}^{\tau + kT_s + T_R} r(t) \hat{\tilde{p}}_R(t; \tau_1) dt,$$

$$k = 0, 1, \cdots, K - 1, \tag{13}$$

where T_R is the nonzero time-support of $p_R(t)$, measured possibly via channel sounding. The peak amplitude of $\mathrm{E}\{y_k^2(\tau)\}$ corresponds to $\tau = \tau_1$, leading to the following timing estimator based on the sample mean square (SMS):

$$\hat{\tau}_1 = \arg \max_{\tau \in [0, T_s]} z(\tau) := \mathrm{E}\left\{ y_k^2(\tau) \right\}. \tag{14}$$

In practice, the sample mean-square is replaced by its consistent sample square average formed by averaging over K symbol periods: $\hat{z}(\tau) = (1/K) \sum_{k=1}^{K} y_k^2(\tau)$.

To understand how this estimator works, let us first examine the data-aided case where we choose the training sequence to consist of binary symbols with alternating signs. Let $\tau_\Delta := [(\tau - \tau_1) \mod T_s]$ denote the closeness of the candidate time-shift τ to the true TOA value τ_1. Within any T_s-long interval, $r(t)$ always contains up to two consecutive symbols. As such, the symbol-rate correlation output $y_k(\tau)$, $\forall \tau$, can be derived from (13) as

$$y_k(\tau) = \int_{\tau + kT_s}^{\tau + kT_s + T_R} \left[\mathcal{E} \sum_{k=0}^{\infty} s[k] p_R^2(t - kT_s - \tau_1) \right] dt$$

$$+ n_k(\tau)$$

$$= \pm \mathcal{E}\left[\mathcal{E}_+(\tau) - \mathcal{E}_-(\tau) \right] + n_k(\tau), \tag{15}$$

where $\mathcal{E}_+(\tau) := \int_{\tau_\Delta}^{T_R} p_R^2(t) dt$ and $\mathcal{E}_-(\tau) := \int_0^{\tau_\Delta + T_R - T_s} p_R^2(t) dt$ are the portions of receive-pulse energy captured from the two contributing symbols within the corresponding T_s-long correlation window. Because $\mathcal{E}_+(\tau)$ and $\mathcal{E}_-(\tau)$ correspond respectively to two adjacent symbols of the pattern $\pm(1, -1)$, they show up in (15) with opposite signs. The $\pm$ sign in (15) is determined by the symbol signs within the correlation window and is irrelevant to the search algorithm in (14). The noise component $n_k(\tau)$ contains two noise terms and one noise-product term contributed from both the noisy signal $r(t)$ and

the noisy template $\hat{\bar{p}}_R(t; \tau_1)$ in (13). In the noise-free case, when $\tau = \tau_1$, we have $\mathcal{E}_+(\tau_1) = \mathcal{E}_{\max} := \int_0^{T_R} p_R^2(t)dt$ and $\mathcal{E}_-(\tau_1) = 0$ by definition. Since the integration range encompasses exactly one symbol, each sample amplitude is determined by the energy $\mathcal{E}_{\max}$ contained in the entire aggregate receive-pulse $p_R(t)$. When $\tau \neq \tau_1$, two consecutive symbols of the pattern $\pm(1, -1)$ contribute to the correlation in (13) with opposite signs, which leads to $|\mathcal{E}_+(\tau) - \mathcal{E}_-(\tau)| < \mathcal{E}_{\max}, \forall \tau \neq \tau_1$, reflecting the energy cancellation effect of this training pattern in the presence of mistiming. This phenomenon explains why the peak amplitude of $z(\tau)$ yields the correct timing estimate for τ_1. The validity of this algorithm can be established even in the presence of noise, as the noise term does not alter the peak location of $z(\tau)$ statistically. It is the change of symbol signs exhibited in the alternating symbol pattern $(1, -1)$ that reveals the timing information in symbol-rate samples [38]. The same timing estimation principle also applies to the non-data-aided case, except that it may take a longer synchronization time for the algorithm to converge; see [15] for detailed derivations.

The SMS estimator in (14) enables timing synchronization at any desirable resolution constrained only by the affordable complexity: i) coarse timing with low complexity, e.g., by picking the maximum over N_f candidate offsets $\{\tau = nT_f\}_{n=0}^{N_f-1}$ taken every T_f in $[0, T_s)$; ii) fine timing with higher complexity at the chip resolution; and iii) adaptive timing (tracking) with voltage-controlled clock (VCC) circuits. As Figure 4 illustrates, the search step size affects the TOA estimation accuracy at the high SNR region, where a smaller stepsize results in a lower error floor. In the low SNR region, the timing accuracy is dominantly dictated by the multipath energy capture capability of the synchronizer, which is independent of the step size thanks to the asymptotically optimal template $\hat{\bar{p}}_R(t; \tau_1)$ used. In a short synchronization time (small K), a reasonable SNR can lead to a low normalized mean-square error (MSE) of 0.3×10^{-3}, which translates into position accuracy of a meter, and can be further improved by a finer scale search.

VARIANCE OF LOW-COMPLEXITY TOA ESTIMATORS

To benchmark timing estimation accuracy of the SMS-based TOA estimator in (14), we now present its asymptotic estimation variance analytically, using first-order perturbation analysis. Because of noise, the maximum of $\hat{z}(\tau)$ moves from τ_1 to $\hat{\tau}_1 = \tau_1 + \Delta\tau$, thus inducing an estimation error $\Delta\tau$. Let $\dot{\hat{z}}(\tau) := \partial\hat{z}(\tau)/\partial\tau$ and $\ddot{z}(\tau) := \partial^2 z(\tau)/\partial\tau^2$ denote the derivatives of the objective function with respect to τ. When the sample size K or transmit SNR $\mathcal{E}$ is sufficiently large such that $|\Delta\tau| \leq \epsilon$, we can use the *mean value theorem* to obtain

$$\dot{\hat{z}}(\hat{\tau}_1) \approx \dot{\hat{z}}(\tau_1 + \Delta\tau) = \dot{\hat{z}}(\tau_1) + \ddot{z}(\tau_1 + \mu\Delta\tau)\Delta\tau, \quad (16)$$

where $\mu \in (0, 1)$ is a scalar that depends on $\Delta\tau$. Because $\dot{\hat{z}}(\hat{\tau}_1) = 0$ and $\ddot{z}(\tau)$ is deterministic, it follows that

$$\Delta\tau = -\frac{\dot{\hat{z}}(\tau_1)}{\ddot{z}(\tau_1 + \mu\Delta\tau)},$$

$$\text{and } \operatorname{var}\{\hat{\tau}_1\} = E\left\{(\Delta\tau)^2\right\} = \frac{E\left\{\dot{\hat{z}}^2(\tau_1)\right\}}{\ddot{z}^2(\tau_1 + \mu\Delta\tau)}. \quad (17)$$

To execute the derivations required by (17), we note that $p_R(t)$, a key component in $z(\tau)$, has finite time support and may not be differentiable at $t = 0$ and $t = T_R$. The following operational condition needs to be imposed:

■ C1: $p_R(t)$ is twice continuously differentiable over $[0, +\epsilon] \cup [T_R - \epsilon, T_R]$, where $\epsilon > 0$ is very small.

Skipping the tedious derivation procedure for conciseness, we bound the MSE of the unbiased timing estimate $\hat{\tau}_1$ as

$$\operatorname{var}\{\Delta\tau^2\} \leq \frac{(BT_R)^2}{2KK_1(2\mathcal{E}/\mathcal{N}_0)^2\Gamma_p}, \quad (18)$$

where

$$\Gamma_p := \min\left\{p_R^2(\mu\Delta\tau)\left[p_R^3(\mu\Delta\tau) - p_R'(\mu\Delta\tau)\mathcal{E}_{\max}\right]^2,\right.$$
$$\left. p_R^2(T_R - \mu\Delta\tau)\left[p_R^3(T_R - \mu\Delta\tau) - p_R'(T_R - \mu\Delta\tau)\mathcal{E}_{\max}\right]^2\right\}$$

is a quantity selected from the worse case between $\tau \geq \tau_1$ and $\tau \leq \tau_1$. Obviously, the timing accuracy of this SMS synchronizer is closely related to $p_R(t)$ via Γ_p. To ensure Γ_p will be positive, the expression in (18) is valid to a limited class of $p_R(t)$ waveforms with the following local behavior around their edges:
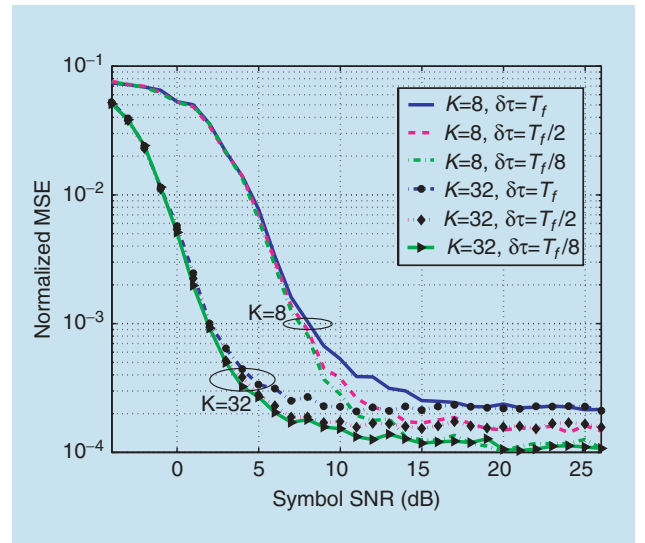
[FIG4] Normalized MSE ($\mathbf{E}\{(|\hat{\tau}_1 - \tau_1|/\mathbf{T_s})^2\}$) of the TOA estimate obtained from (14): *K* is the number of training symbols used and $\delta\tau$ is the search stepsize for candidate τs. Simulation parameters are: $N_f = 20$, $T_f = 50$ ns, $T_p = T_c = 1$ ns, $N_c = $ **48 with randomly generated TH code, and a typical UWB multipath channel modeled by [48] with parameters $\Lambda = 0.5$ ns, $\lambda = 2$ ns, $\Gamma = 30$ ns, and $\gamma = 5$ ns.**

- C2: $p_R(t) \propto t^a$ in $t \in [0, +\epsilon]$, with $-1/2 < a < 1/2$,
- C3: $p_R(t) \propto (T_R - t)^b$ in $t \in [T_R - \epsilon, T_R]$, with $-1/2 < b < 1/2$.

The result in (18) delineates the required K (and K_1) to achieve a desired level of timing accuracy for a practical positioning system. On the other hand, the asymptotic variance is applicable only under conditions C1–C3 for a small-error local region around τ_1, which requires the search time resolution to be sufficiently small and the SNR or K to be sufficiently large. In general, the TOA estimation accuracy decreases as the time-bandwidth product BT_R increases, but it can be markedly improved either by more averaging (larger K or K_1) or by higher SNR.

FUNDAMENTAL LIMITS FOR LOCATION ESTIMATION

In the previous section, we have considered the theoretical limits for TOA estimation. This section considers the limits for the location estimation problem. We first consider location estimation based on TOA measurements and then location estimation based on TOA and SS measurement. The receiver structures for asymptotically achieving those limits will also be discussed [32].

FUNDAMENTAL LIMITS FOR TOA-BASED LOCATION ESTIMATION

Consider a synchronous system with N nodes, M of which have NLOS to the node they are trying to locate, while the remaining ones have LOS. Suppose that we know a priori which nodes have LOS and which have NLOS. This can be obtained by employing NLOS identification techniques [61]–[63]. When such information is unavailable, all first arrivals can be treated as NLOS signals.

The received signal at the ith node can be expressed as

$$ r_i(t) = \sum_{l=1}^{L_i} \alpha_{il} s(t - \tau_{il}) + n_i(t), \qquad (19) $$

for $i = 1, \ldots, N$, where L_i is the number of multipath components at the ith node, α_{il} and τ_{il} are the respective amplitude and delay of the lth path of the ith node, $s(t)$ is the UWB signal as in (5), and $n_i(t)$ is a zero mean AGWN process with spectral density $\mathcal{N}_0/2$. We assume, without loss of generality, that the first M nodes have NLOS and the remaining $N - M$ have LOS.

For a 2-D location estimation problem, the delay τ_{ij} in (19) can be expressed as

$$ \tau_{ij} = \frac{1}{c}\left[\sqrt{(x_i - x)^2 + (y_i - y)^2} + l_{ij}\right], \qquad (20) $$

> **TIME-BASED POSITIONING TECHNIQUES RELY ON MEASUREMENTS OF TRAVEL TIMES OF SIGNALS BETWEEN NODES.**

for $i = 1, \ldots, N$, $j = 1, \ldots, L_i$, where $c = 3 \times 10^8$ m/s is the speed of light, $[x_i, y_i]$ is the location of the ith node, l_{ij} is the extra path length induced by NLOS propagation, and $[x, y]$ is the target location to be estimated.

Note that $l_{i1} = 0$ for $i = M + 1, \ldots, N$ since the signal directly reaches the related node in a LOS situation. Hence, the parameters to be estimated are the NLOS delays and the location of the node, $[x, y]$, which can be expressed as $\boldsymbol{\theta} = [x \; y \; \boldsymbol{l}_{M+1} \cdots \boldsymbol{l}_N \; \boldsymbol{l}_1 \cdots \boldsymbol{l}_M]$, where

$$ \boldsymbol{l}_i = \begin{cases} (l_{i1} \; l_{i2} \cdots l_{iL_i}) & \text{for } i = 1, \ldots, M, \\ (l_{i2} \; l_{i3} \cdots l_{iL_i}) & \text{for } i = M + 1, \ldots, N, \end{cases} \qquad (21) $$

with $0 < l_{i1} < l_{i2} \cdots < l_{iN_i}$ [32]. Note that for LOS signals the first delay is excluded from the parameter set since these are known to be zero.

From (19), the joint probability density function (pdf) of the received signals from the N reference nodes, $\{r_i(t)\}_{i=1}^N$, can be expressed, conditioned on $\boldsymbol{\theta}$, as follows:

$$ f_{\boldsymbol{\theta}}(r) \propto \prod_{i=1}^N \exp\left\{-\frac{1}{\mathcal{N}_0}\int \left| r_i(t) - \sum_{j=1}^{L_i} \alpha_{ij} s(t - \tau_{ij}) \right|^2 dt\right\}. \qquad (22) $$

From the expression in (22), the lower bound on the variance of any unbiased estimator for the unknown parameter $\boldsymbol{\theta}$ can be obtained. Toward that end, the FIM can be obtained as [32]

$$ \mathbf{J}_{\boldsymbol{\theta}} = \frac{1}{c^2} \mathbf{H} \mathbf{J}_\tau \mathbf{H}^T, \qquad (23) $$

where

$$ \mathbf{H} := \begin{bmatrix} \mathbf{H}_{\mathrm{NLOS}} & \mathbf{H}_{\mathrm{LOS}} \\ \mathbf{I} & \mathbf{0} \end{bmatrix} \text{ and } \mathbf{J}_\tau := \begin{bmatrix} \boldsymbol{\Lambda}_{\mathrm{NLOS}} & \mathbf{0} \\ \mathbf{0} & \boldsymbol{\Lambda}_{\mathrm{LOS}} \end{bmatrix}, $$

with $\tau := [\tau_{11} \cdots \tau_{1L_1} \cdots \tau_{N1} \cdots \tau_{NL_N}]$. Matrices $\mathbf{H}_{\mathrm{NLOS}}$ and $\mathbf{H}_{\mathrm{LOS}}$ are related to NLOS and LOS nodes, respectively, and depend on the angles between the target node and the reference nodes [32]. The components of $\mathbf{J}_\tau$ are given by $\boldsymbol{\Lambda}_{\mathrm{NLOS}} := \mathrm{diag}\{\boldsymbol{\Psi}_1, \boldsymbol{\Psi}_2, \ldots, \boldsymbol{\Psi}_M\}$ and $\boldsymbol{\Lambda}_{\mathrm{LOS}} := \mathrm{diag}\{\boldsymbol{\Psi}_{M+1}, \boldsymbol{\Psi}_{M+2}, \ldots, \boldsymbol{\Psi}_N\}$, where

$$ [\boldsymbol{\Psi}_i]_{jk} = \frac{2\alpha_{ij}\alpha_{ik}}{\mathcal{N}_t} \int \frac{\partial}{\partial \tau_{ij}} s(t - \tau_{ij}) \frac{\partial}{\partial \tau_{ik}} s(t - \tau_{ik}) dt, \qquad (24) $$

for $j \neq k$, and $[\boldsymbol{\Psi}_i]_{jj} = 8\pi^2 \beta^2 SNR_{ij}$, where $SNR_{ij} = (|\alpha_{ij}|^2/\mathcal{N}_0)$ is the signal to noise ratio of the jth multi-

path component of the ith node's signal, assuming that $s(t)$ has unit energy and β is given as in (3).

The CRLB for the location estimation problem is the inverse of the FIM matrix; that is, $E_{\boldsymbol{\theta}}\{(\hat{\boldsymbol{\theta}} - \boldsymbol{\theta})(\hat{\boldsymbol{\theta}} - \boldsymbol{\theta})^T\} \geq J_{\boldsymbol{\theta}}^{-1}$. It can be shown that the first $a \times a$ block of the inverse matrix is given by [32]

$$\left[J_{\boldsymbol{\theta}}^{-1} \right]_{a \times a} = c^2 \left(H_{\text{LOS}} \boldsymbol{L}_{\text{LOS}} H_{\text{LOS}}^T \right)^{-1}, \qquad (25)$$

where $a := 2 + \sum_{i=M+1}^{N}(L_i - 1)$. Since the main unknown parameters to be estimated, x and y, are the first two elements of $\boldsymbol{\theta}$, (25) proves that the CRLB depends only on the signals from the LOS nodes. Note that we do not assume any statistical information about the NLOS delays in this case.

Moreover, the numerical examples in [32] show that, in most cases, the CRLB is almost the same whether we use all the multipath components from the LOS nodes, or just the first arriving paths of the LOS nodes. For very large bandwidths, the ML estimator for the node location that uses the first arriving paths from the LOS nodes becomes asymptotically optimal [32], which suggests that, for UWB systems, only the first arriving signals from the LOS nodes are sufficient for an asymptotically optimal receiver design. This receiver, shown in Figure 5, can be implemented by the following steps.
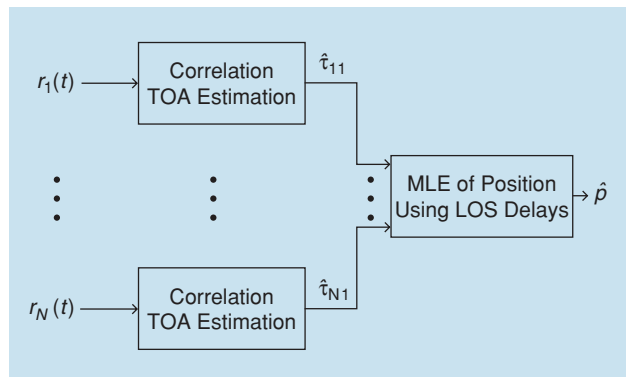
■ Estimate the delays of the first multipath components; solutions are available either via the SMS synchronizer in (14) and those in [34]–[38] or by correlation techniques in which each reference node selects the delay corresponding to the maximum correlation between the received signal and a receive-waveform template [32].

■ Obtain the ML estimate for the position of the target node using the delays of the first multipath components of the LOS nodes.

In other words, the first step of the optimal receiver, the estimation of the first signal path, can be considered separately from the overall positioning algorithm without any loss in optimality.

To use the closed-form CRLB expressions above, consider the simple positioning scenario in Figure 6, where the target node is in the middle of six reference nodes located uniformly around a circle. In Figure 7, the minimum positioning error, defined as $\sqrt{\text{trace}([J_{\boldsymbol{\theta}}^{-1}]_{2 \times 2})}$, is plotted against the effective bandwidth for different numbers of NLOS nodes, M, at SNR $= 0$ dB. The channels between the target and the reference nodes have ten taps that are independently generated from a lognormally distributed fading model with random signs and exponentially decaying tap energy. It can be observed that the large bandwidth of the UWB signals makes it possible to obtain location estimates with very high accuracy.

When there is statistical information about the NLOS delays, where the pdf for node i is denoted by $p_{l_i}(l_i)$ for $i = 1, \ldots, N$, the lower bound of the estimation error is expressed by the generalized CRLB (G-CRLB) $E_{\boldsymbol{\theta}}\{(\hat{\boldsymbol{\theta}} - \boldsymbol{\theta})(\hat{\boldsymbol{\theta}} - \boldsymbol{\theta})^T\} \geq (J_{\boldsymbol{\theta}} + J_P)^{-1}$, where

$$J_P = E \left\{ \frac{\partial}{\partial \boldsymbol{\theta}} \ln p_{\boldsymbol{\theta}}(\boldsymbol{\theta}) \left(\frac{\partial}{\partial \boldsymbol{\theta}} \ln p_{\boldsymbol{\theta}}(\boldsymbol{\theta}) \right)^T \right\}, \qquad (26)$$

[FIG5] An asymptotically optimum receiver structure for positioning. No information about the statistics of the NLOS delays is assumed.
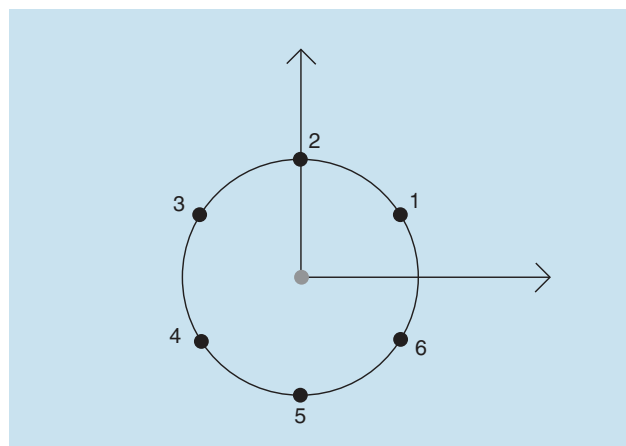
[FIG6] A simple location estimation scenario, where six reference nodes are trying to locate the target node in the middle.
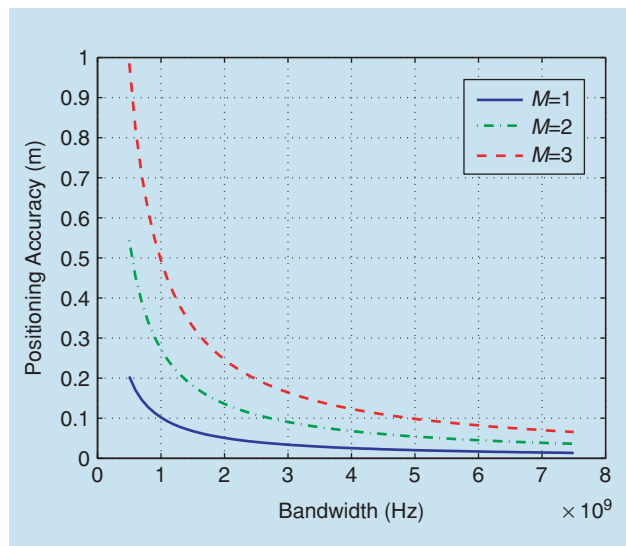
[FIG7] Minimum positioning error versus bandwidth for different number of NLOS nodes. For $M = 1$, node 1; for $M = 2$, node 1 and 1; and for $M = 3$, node 1, 2, and 3 are the NLOS nodes. The UWB channels are modeled as in [64] with $L = 10$, $\lambda = 0.25$ and $\sigma^2 = 1$.

with the expectation being taken over θ [65]. Note that $p_\theta(\theta) = \prod_{i=1}^N p_{l_i}(l_i)$ since it is assumed that multipath delays at different nodes are independent and the other parameters in θ, namely x, y, and l_0 are constant unknown parameters.

Under some conditions, the MAP estimator based on time-delay estimates from all available multipath components is asymptotically optimal [32]. In other words, unlike the case where no NLOS information exists, the accuracy depends on the delay estimates from all the nodes in the presence of statistical NLOS information.

When UWB systems are considered, the large number of multipath components makes it very costly to implement the optimal location estimation algorithm. However, as observed by the numerical analysis in [32], only the strongest multipath components provide substantial improvement in the estimation accuracy. Therefore, simpler suboptimal algorithms that make use of a few strongest multipath components can provide satisfactory performance at lower cost.

HYBRID LOCATION ESTIMATION FOR UWB SYSTEMS
Although SS measurements are easily available since mobile terminals constantly monitor the strength of neighboring base stations' pilot signals for handoff purposes [66], [67], the SS ranging technique is not very accurate in cellular networks because of its dependency on the distance of a located device to reference devices (i.e., base stations). On the other hand, the results in [22] indicate that in short-range wideband communications, the use of received signal strength measurements in conjunction with TOA or TDOA leads to two enhancements in positioning with respect to the case where only TOA or TDOA measurements are used: improved overall location estimation accuracy and significantly lower CRLB within close proximity of the SS devices and suppression of singularities in the CRLB when closer to TOA devices.

> **UWB TECHNOLOGY PROVIDES AN EXCELLENT MEANS FOR WIRELESS POSITIONING DUE TO ITS HIGH RESOLUTION CAPABILITY IN THE TIME DOMAIN.**

In sensor networks, the distances between sensor nodes and the neighboring reference devices are on the order of tens of meters. For example, in the emerging ZigBee standards, which relies on the IEEE 802.15.4 MAC/PHY, the typical transmission range is 15–30 m. Therefore, TDOA/SS and TOA/SS hybrid positioning schemes may achieve better positioning accuracy.
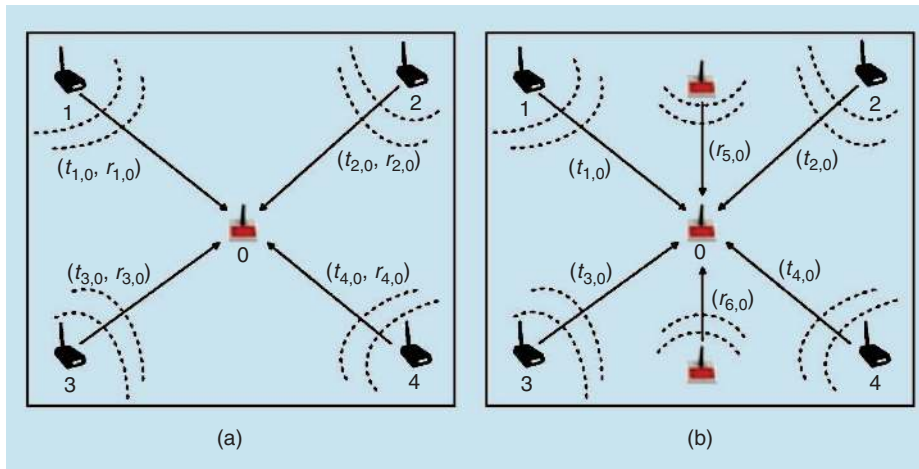
MODELING TOA AND SS OBSERVATIONS
The TOA observations $t_{i,j}$ between devices i and j are commonly modeled as normal random variables $t_{i,j} \sim \mathcal{N}(d_{i,j}/c, \sigma_T^2)$ [68], where $d_{i,j}$ is the separation of the two devices, c is the speed of radio-wave propagation, and σ_T is the parameter describing the joint nuisance parameters of the multipath channel and the measurement error. On the other hand, the SS measurements are conventionally modeled as log-normal random variables and can be expressed in decibels as $r_{i,j} \sim \mathcal{N}(P_{dB}^{ir}, \sigma_{sh}^2)$, with $P_{dB}^{ir} = P_{dB}^{jt} - 10 n_p \log_{10}(d_{i,j})$, where P_{dB}^{ir} and P_{dB}^{jt} are the decibel values of the mean received power at device i and the mean transmitted power at device j, respectively, n_p is the propagation exponent, and σ_{sh}^2 is the variance of the log-normal shadowing. In UWB channel modeling, frequency dependence of the path loss has also been reported [69] and appears to be independent of the distance dependent losses; i.e.,

$$P_{dB,uwb}^{ir} = P_{dB}^{ir}(d_{i,j}) + P_{dB}^{ir}(f). \tag{27}$$

The positive bias in the mean received power due to the frequency, f, can be assumed to be deterministic and known through measurements.

HYBRID OBSERVATIONS AND THE CRLB
In a positioning scheme that relies on both TOA and SS measurements, a device may track the TOA and SS of incoming signals from a single transmitter as illustrated in Figure 8(a). These measurements may also be obtained separately from different transmitters as in Figure 8(b). If discrepancy in communication ranges exists between a transmitter-receiver pair, it is very likely that round-trip TOA cannot be acquired, but a TDOA can become available from two such transmitters. In these cases, additional information to enhance positioning accuracy can still be obtained from SS measurements from neighboring nodes.


[FIG8] Illustration of different hybrid TOA and SS observation scenarios.

Let S_0 denote a node whose location is being estimated, and assume that there are N reference nodes within communication range of S_0, of which N_{TOA} nodes perform TOA and N_{SS} provide SS measurements such that $N = N_{TOA} + N_{SS}$. Also assume that the actual coordinate vector of S_0 is $\boldsymbol{\theta}_0 = [x_0 \; y_0]$ and denote its estimate by $\hat{\boldsymbol{\theta}}_0$. Then, the location estimation problem is to find $\hat{\boldsymbol{\theta}}_0$, given the coordinate vector of the reference devices, $\boldsymbol{\theta} = [\theta_1 \; \theta_2 \cdots \theta_N]$.

The CRLB of an unbiased estimator $\hat{\boldsymbol{\theta}}_0$ is $\mathrm{Cov}(\hat{\boldsymbol{\theta}}_0) \geq \mathbf{J}_{\boldsymbol{\theta}_0}^{-1}$, where $\mathbf{J}_{\boldsymbol{\theta}_0}$ is the FIM. The CRLB of the TOA/SS hybrid location estimation scheme is given in [22]. Here we generalize it to the following closed-form expression based on the problem statement defined earlier (see (28) at the bottom of the page) where $b = (10 n_p / \sigma_{sh} \log 10)^2$ and $A_{i,j} = (d_{i,j} d_{0 \perp (i,j)} / d_{i,0} d_{j,0})$ is a unitless parameter called the "geometric conditioning" of devices i and j with respect to S_0. The parameter $d_{0 \perp (i,j)}$ is the length of the shortest distance between S_0 and the line that connects i and j as shown in Figure 9.

The denominator in (28) consists of three expressions: the contribution of the TOA measurements only, which is a function of the geometric conditioning of TOA devices with respect to S_0; the geometric conditioning of the TOA and SS reference devices with respect to S_0; and the contribution of the SS measurements alone, which is determined by the separation of S_0 from the SS reference nodes. It is clear from (28) that besides the number of TOA and SS devices in the network, how they are placed relative to one another also determines the level of CRLB. For instance, as illustrated in Figure 10(a), placed at two corners of a 100×100 meter field are two TOA devices and at coordinates $(25, 25), (50, 50)$, and $(75, 75)$ are three SS devices. The $\sqrt{\mathrm{CRLB}}$ is given in the case of $\sigma_T = 6$ ns and $\sigma_{sh}/n = 2$. These values are determined from wideband field measurements reported in [68]. Within close proximity of SS devices, the bound is lowered; and at locations closer to a TOA device it gets worse. In Figure 10(b), the positions of the SS devices are moved to the coordinates $(25, 75), (50, 50)$, and $(75, 25)$ such that all the TOA and SS devices are aligned along a diagonal, causing the CRLBs to be adversely affected. The geometric conditioning of S_0 with respect to a TOA and an SS device becomes zero, when they are all aligned along a line. This expectedly lowers the numerical value that the middle term of the denominator in (28) would generate, unless some SS devices are placed off the line to have nonzero contributions [Figure 10(a)]. Therefore, the CRLB gets relatively higher within close proximity of the aligned nodes. To lower the bound, one should avoid forming a straight line with two or more SS devices and a TOA device. Similarly, the same design rule should be advocated among TOA devices, if there exist more than one of them within communication range of S_0.

In the TDOA/SS case, a TDOA observation is derived from two TOA observations as their difference, sacrificing an independent TOA measurement. Therefore, a TDOA observation at S_0 from
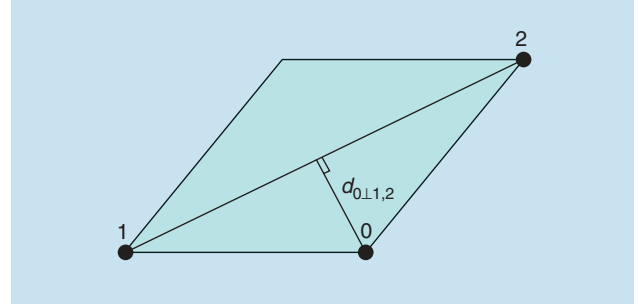
[FIG9] Illustration of the geometric conditioning of devices 1 and 2 with respect to 0, $A_{i,j} = (d_{i,j} d_{0 \perp (i,j)} / d_{i,0} d_{j,0})$.

any two terminals i and j can be modeled as $\tau_{i,j} \sim \mathcal{N}((d_{i,0} - d_{j,0})/c, \, 2\sigma_T^2)$. Note that $N_{TDOA} = N_{TOA} - 1$, and consequently the variance increases.

CONCLUSIONS

UWB technology provides an excellent means for wireless positioning due to its high resolution capability in the time domain. Its ability to resolve multipath components makes it possible to obtain accurate location estimates without the need for complex estimation algorithms. This precise location estimation capability facilitates many applications such as medical monitoring, security, and asset tracking. Standardization efforts are underway in the IEEE 802.15.4a PAN standard, which will make use of the unique features of the UWB technology for location-aware sensor networking. In this article, theoretical limits for TOA estimation and TOA-based location estimation for UWB systems have been considered. Due to the complexity of the optimal schemes, suboptimal but practical alternatives have been emphasized. Performance limits for hybrid TOA/SS and TDOA/SS schemes have also been considered.

Although the fundamental mechanisms for localization, including AOA-, TOA-, TDOA-, and SS-based methods, apply to all radio air interface, some positioning techniques are favored by UWB-based systems using ultrawide bandwidths. Due to the high time resolution of UWB signals, time-based location estimation schemes usually provide better accuracy than the others. To implement a time-based scheme, the TOA estimation algorithm based on noisy templates can be employed, which is a very suitable approach for UWB systems due to its excellent multipath energy capture capability at affordable complexity. In the cases where certain nodes in the network can measure only signal strength (such as the biomedical sensing nodes in a body area network), the use of hybrid TOA/SS or TDOA/SS schemes can be useful for obtaining accurate location estimates.

$$\sigma_{CRLB}^2 = \frac{\frac{N_{TOA}}{c^2 \sigma_T^2} + b \sum_{i=1}^{N_{SS}} d_{i,0}^2}{\frac{1}{(c^2 \sigma_T^2)^2} \sum_{i=1}^{N_{TOA}} \sum_{\substack{j=1 \\ i<j}}^{N_{TOA}} A_{i,j}^2 + \frac{b}{c^2 \sigma_T^2} \sum_{i=1}^{N_{TOA}} \sum_{j=1}^{N_{SS}} \frac{A_{i,j}^2}{d_{j,0}^2} + b^2 \sum_{i=1}^{N_{SS}} i < j \sum_{\substack{j=1 \\ i<j}}^{N_{SS}} \left(\frac{A_{i,j}}{d_{i,0} \, d_{j,0}} \right)^2}, \qquad (28)$$
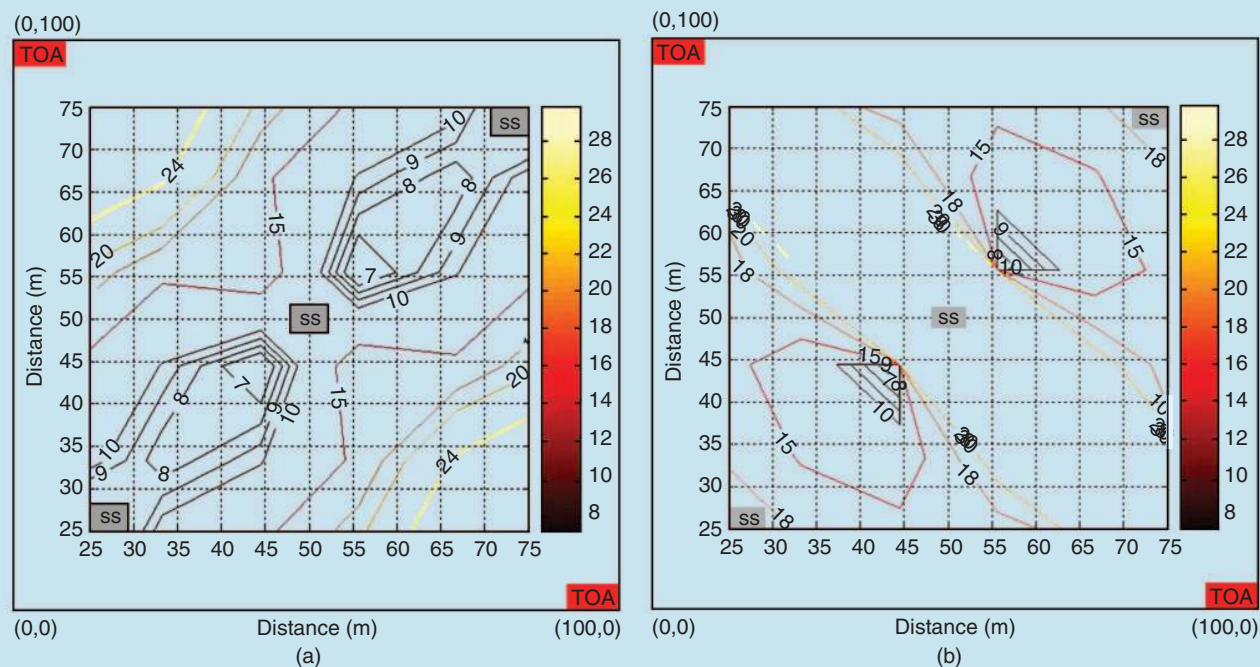
[FIG10] The $\sqrt{\text{CRLB}}$ versus different node positions in the case of $\sigma_T = 6$ ns and $\sigma_{sh}/n = 2$.

AUTHORS

Sinan Gezici received the B.S. degree from Bilkent University, Turkey, in 2001 and the M.A. degree from Princeton University in 2003. He is currently working toward the Ph.D. degree at the Department of Electrical Engineering at Princeton University. His research interests are in the communications and signal processing fields. He has a particular interest in synchronization, positioning, performance analysis, and multiuser aspects of ultra wideband communications.

Zhi Tian received the B.E. degree in electrical engineering (automation) from the University of Science and Technology of China, Hefei, in 1994 and the M.S. and Ph.D. degrees from George Mason University, Fairfax, Virginia, in 1998 and 2000. From 1995 to 2000, she was a graduate research assistant in the Center of Excellence in Command, Control, Communications, and Intelligence (C3I) of George Mason University. Since August 2000, she has been an assistant professor with the Department of Electrical and Computer Engineering, Michigan Technological University. Her current research focuses on signal processing for wireless communications, particularly on ultra-wideband systems. She is an associate editor for *IEEE Transactions on Wireless Communications*. She is the recipient of a 2003 NSF CAREER award and is a Member of the IEEE.

Georgios B. Giannakis received his diploma in electrical engineering from the National Technical University of Athens, Greece, in 1981. From the University of Southern California, he received his M.Sc. in electrical engineering (1983), M.Sc. in mathematics (1986), and Ph.D. in electrical engineering (1986). He joined the University of Virginia in 1987, where he became a professor of electrical engineering in 1997. Since 1999 he has been a professor with the Department of Electrical and Computer Engineering at the University of Minnesota, where he now holds the ADC Chair in Wireless Telecommunications. His general interests span the areas of communications and signal processing, estimation and detection theory, time-series analysis, and system identification, subjects on which he has published more than 200 journal papers, 350 conference papers, and two edited books. He is the (co-)recipient of six paper awards from the IEEE Signal Processing and IEEE Communications Societies. He also received the IEEE Signal Processing Society's Technical Achievement Award in 2000. He is a Fellow of the IEEE.

Hisashi Kobayashi has been the Sherman Fairchild University Professor at Princeton University since 1986, when he joined the university as dean of the Engineering School. He was founding director of IBM Tokyo Research Lab . Prior to that he held several managerial positions at IBM Research Center in Yorktown Heights, New York. He received B.E and

M.E degrees from University of Tokyo in 1961 and 1963, and worked for Toshiba, Japan. He came to Princeton as Orson Desaix Munn Fellow in 1965 and received his Ph.D. in 1967. He is the inventor of high-density digital recording technique, known as "PRML (partial response, maximum likelihood)" and the co-inventor (with L. R. Bahl) of "relative address coding." His current research interest includes network security and ultra-wideband. He is a Life Fellow of the IEEE and a Fellow of IEICE, Japan. He received the 1979 Humboldt Prize from Germany and 1980 IFIP Silver Core and was elected to the Engineering Academy of Japan.

Andreas F. Molisch received the Dipl. Ing. and Dr. techn. degrees from the Technical University (TU) Vienna, Austria, in 1990 and 1994, respectively. From 1991 to 2000, he was with the TU Vienna, and from 2000–2002, he was with AT&T Labs–Research. Since then, he has been a senior principal member of technical staff with Mitsubishi Electric Research Labs, Cambridge, Massachusetts. He is also professor and chairholder for radio systems at Lund University, Sweden. His current research interests are MIMO systems, measurement and modeling of mobile radio channels, and ultra-wideband. He has authored, co-authored, or edited two books, eight book chapters, some 85 journal papers, and numerous conference contributions. He is an editor of *IEEE Transactions on Wireless Communications*, coeditor of an upcoming special issue of *IEEE Journal in Selected Areas in Communications* on ultra wideband, and vice-chair of the TPC of the 2005 IEEE Vehicular Technology Conference. He is the chair of the COST273 and IEEE 802.15.4a channel modeling groups and vice chairman of Commission C of URSI (International Union of Radio Scientists). He is a Fellow of the IEEE and the recipient of several awards.

H. Vincent Poor received the Ph.D. degree in electrical engineering and computer science from Princeton University in 1977. From 1977 until 1990, he was on the faculty of the University of Illinois at Urbana-Champaign. Since 1990 he has been on the faculty at Princeton, where he is the George Van Ness Lothrop Professor in Engineering. His research interests are in the areas of wireless networks, advanced signal processing, and related fields. Among his publications is the recent book *Wireless Networks: Multiuser Detection in Cross-Layer Design*. He is a Fellow of the IEEE, the American Academy of Arts and Sciences, and other organizations. He is a past President of the IEEE Information Theory Society and is editor-in-chief of *IEEE Transactions on Information Theory*. Recent recognition of his work includes the 2002 NSF Director's Award, a Guggenheim Fellowship, and the 2005 IEEE Education Medal.

Zafer Sahinoglu received his B.S. in electrical engineering from Gazi University, Turkey, M.S. in biomedical engineering and Ph.D. (with awards) in electrical engineering from New Jersey Institute of Technology (NJIT) in 1998 and 2001, respectively. He worked at AT&T Shannon Research Labs in 1999 and has been with MERL since 2001. His current research interests include heterogeneous wireless sensor networks and ultra-wideband ranging and positioning. He has coauthored a book-chapter on UWB geolocation, and has been author and co-author of more than 24 conference and journal articles; he has provided significant contributions to emerging MPEG-21 standards on mobility modeling and characterization for multimedia service adaptation, to ZigBee on data broadcasting, routing and application profile development, to IEEE 802.15.4a standards on precision ranging. He is currently the chair of ZigBee Industrial Plant Monitoring Application Profile Task Group and a vice technical editor for ranging part of IEEE 802.15.4a. He holds one European and three U.S. patents and has 17 pending. He is a Member of the IEEE.

REFERENCES

[1] M.Z. Win and R.A. Scholtz, "On the energy capture of ultra-wide bandwidth signals in dense multipath environments," *IEEE Commun. Lett.*, vol. 2, pp. 245–247, Sept. 1998.

[2] M.L. Welborn, "System considerations for ultra-wideband wireless networks," in *Proc. IEEE Radio and Wireless Conf. 2001*, Boston, MA, Aug. 2001, pp. 5–8.

[3] J.D. Taylor, Ed., *Introduction to Ultra-Wideband Radar Systems*. Boca Raton, FL: CRC Press, 1995.

[4] M.G.M. Hussain, "Ultra-wideband impulse radar—An overview of the principles," *IEEE Aerosp. Electron. Syst. Mag.*, vol. 13, no. 9, pp. 9–14, 1998.

[5] R.A. Scholtz, "Multiple access with time-hopping impulse modulation Scholtz," in *Proc. IEEE Military Communications Conf. (MILCOM'93)*, Bedford, MA, Oct. 1993, vol. 2, pp. 447–450.

[6] M.Z. Win and R.A. Scholtz, "Impulse radio: How it works," *IEEE Commun. Lett.*, vol. 2, no. 2, pp. 36–38, Feb. 1998.

[7] M.Z. Win and R.A. Scholtz, "Ultra-wide bandwidth time-hopping spread-spectrum impulse radio for wireless multiple-access communications," *IEEE Trans. Commun.*, vol. 48, no. 4, pp. 679–691, Apr. 2000.

[8] "First Report and Order 02–48," Federal Communications Commission, Washington, DC, 2002.

[9] A.F. Molisch, Y.P. Nakache, P. Orlik, J. Zhang, Y. Wu, S. Gezici, S.Y. Kung, H. Kobayashi, H.V. Poor, Y.G. Li, H. Sheng, and A. Haimovich, "An efficient low-cost time-hopping impulse radio for high data rate transmission," *EURASIP J. Applied Signal Processing*, vol. 2005, no. 3, pp. 397–412, Mar. 2005.

[10] J. Balakrishnan, A. Batra, and A. Dabak, "A multi-band OFDM system for UWB communication," in *Proc. IEEE Conf. Ultra Wideband Systems and Technologies (UWBST'03)*, Reston, VA, Nov. 2003, pp. 354–358.

[11] P. Runkle, J. McCorkle, T. Miller, and M. Welborn, "DS-CDMA: The modulation technology of choice for UWB communications," in *Proc. IEEE Conf. Ultra Wideband Systems and Technologies (UWBST'03)*, Reston, VA, Nov. 2003, pp. 364–368.

[12] S. Roy, J.R. Foerster, V.S. Somayazulu, and D.G. Leeper, "Ultrawideband radio design: The promise of high-speed, short-range wireless connectivity," *Proc. IEEE*, vol. 92, no. 2, pp. 295–311, Feb. 2004.

[13] W. Hirt, "Ultra-wideband radio technology: Overview and future research," *Computer Commun. J.*, vol. 26, no. 1, pp. 46–52, 2003.

[14] W. Zhuang, X.S. Shen, and Q. Bi, "Ultra-wideband wireless communications," *Wireless Commun. Mobile Comput. J.*, vol. 3, no. 6, pp. 663–685, 2003.

[15] L. Yang and G.B. Giannakis, "Ultra-wideband communications: An idea whose time has come," *IEEE Signal Processing Mag.*, vol. 21, no. 6, pp. 26–54, Nov. 2004.

[16] G. Sun, J. Chen, W. Guo, and K.J.R. Liu, "Signal processing techniques in network-aided positioning," *IEEE Signal Processing Mag.*, vol. 22, no. 4, pp. 12–23, July 2005.

[17] F. Gustafsson and F. Gunnarsson, "Mobile positioning using wireless networks," *IEEE Signal Processing Mag.*, vol. 22, no. 4, pp. 41–53, July 2005.

[18] A.H. Sayed, A. Taroghat, and N. Khajehnouri, "Network-based wireless location," *IEEE Signal Processing Mag.*, vol. 22, no. 4, pp. 24–40, July 2005.

[19] N. Patwari, A.O. Hero III, J. Ash, R.L. Moses, S. Kyperountas, and N.S. Correal, "Locating the nodes," *IEEE Signal Processing Mag.*, vol. 22, no. 4, pp. 54–69, July 2005.

[20] J. Caffery, Jr., *Wireless Location in CDMA Cellular Radio Systems*. Boston, MA: Kluwer, 2000.

[21] Y. Qi and H. Kobayashi, "On relation among time delay and signal strength based geolocation methods," in *Proc. IEEE Global Telecommunications Conf. (GLOBECOM'03)*, San Francisco, CA, Dec. 2003, vol. 7, pp. 4079–4083.

[22] Z. Sahinoglu and A. Catovic, "A hybrid location estimation scheme (H-LES) for partially synchronized wireless sensor networks," in *Proc. IEEE Int. Conf. Communications (ICC 2004)*, Paris, France, June 2004, vol. 7, pp. 3797–3801.

[23] H.V. Poor, *An Introduction to Signal Detection and Estimation,* 2nd ed. New York: Springer-Verlag, 1994.

[24] C.E. Cook and M. Bernfeld, *Radar Signals: An Introduction to Theory and Applications*. New York: Academic, 1970.

[25] Y. Shimizu and Y. Sanada, "Accuracy of relative distance measurement with ultra wideband system," in *Proc. IEEE Conf. Ultra Wideband Systems and Technologies (UWBST'03)*, Reston, VA, Nov. 2003, pp. 374–378.

[26] JY. Lee and R.A. Scholtz, "Ranging in a dense multipath environment using an UWB radio link," *IEEE Trans. Select. Areas Commun.,* vol. 20, no. 9, pp. 1677–1683, Dec. 2002.

[27] J.C. Adams, W. Gregorwich, L. Capots, and D. Liccardo, "Ultra-wideband for navigation and communications," in *Proc. IEEE Aerospace Conf.*, Big Sky, MT, Mar. 2001, vol. 2, pp. 785–792.

[28] G.L. Turin, "An introduction to matched filters," *IRE Trans. Inform. Theory*, vol. IT-6, no. 3, pp. 311–329, Jun. 1960.

[29] Y. Qi, "Wireless geolocation in a non-line-of-sight environment," Ph.D. dissertation, Princeton Univ., Princeton, NJ, Nov. 2003.

[30] Y. Qi, H. Kobayashi, and H. Suda, "Unified analysis of wireless geolocation in a non-line-of-sight environment—Part I: Analysis of time-of-arrival positioning methods," submitted for publication.

[31] Y. Qi and H. Kobayashi, "A unified analysis for Cramer-Rao lower bound for geolocation," in *Proc. 36th Ann. Conf. Information Sciences and Systems (CISS 2002)*, Princeton Univ., Princeton, NJ, Mar. 2002, pp. 598–602.

[32] Y. Qi, H. Suda, and H. Kobayashi,, "On time-of arrival positioning in a multipath environment," in *Proc. IEEE 60th Vehicular Technology Conf. (VTC 2004-Fall)*, Los Angeles, CA, Sept. 26–29, 2004, vol. 5, pp. 3540–3544.

[33] M.A. Pallas and G. Jourdain, "Active high resolution time delay estimation for large BT signals," *IEEE Trans. Signal Processing*, vol. 39, no. 4, pp. 781–788, Apr. 1991.

[34] Z. Tian, L. Yang, and G.B. Giannakis, "Symbol timing estimation in ultra wideband communications," in *Proc. IEEE Asilomar Conf. Signals, Systems, and Computers*, Pacific Grove, CA, Nov. 2002, vol. 2, pp. 1924–1928.

[35] Z. Tian and L. Wu, "Timing acquisition with noisy template for ultra-wideband communications in dense multipath," *EURASIP J. Applied Signal Processing*, vol. 2005, no. 3, pp. 439–454, Mar. 2005.

[36] L. Yang and G.B. Giannakis, "Low-complexity training for rapid timing acquisition in ultra-wideband communications," in *Proc. Globecom Conf.*, San Francisco, CA, Dec. 1–5, 2003, vol. 2, pp. 769–773.

[37] L. Yang and G.B. Giannakis, "Blind UWB timing with a dirty template," in *Proc. Int. Conf. Acoustics, Speech and Signal Processing*, Montreal, Quebec, Canada, vol. 4, May 2004, pp. IV.509–512.

[38] Z. Tian and G.B. Giannakis, "A GLRT approach to data-aided timing acquisition in UWB radios—Part I: Algorithms," *IEEE Trans. Wireless Commun.*, to be published.

[39] IEEE 802.15 WPAN Task Group 3 (TG3) [Online]. Available: http://www.ieee802.org/15/pub/TG3.html

[40] M. McGuire, K.N. Plataniotis, and A.N. Venetsanopoulos, "Location of mobile terminals using time measurements and survey points," *IEEE Trans. Veh. Technol.*, vol. 52, no. 4, pp. 999–1011, Jul. 2003.

[41] S. Gezici, H. Kobayashi, and H.V. Poor, "A new approach to mobile position tracking," in *Proc. IEEE Sarnoff Symp. Advances in Wired and Wireless Communications*, Ewing, NJ, Mar. 2003, pp. 204–207.

[42] M.P. Wylie and J. Holtzman, "The non-line of sight problem in mobile location estimation," in *Proc. 5th IEEE Int. Conf. Universal Personal Communications*, Cambridge, MA, Sept. 1996, vol. 2, pp. 827–831.

[43] S. Al-Jazzar and J. Caffery, Jr., "ML and Bayesian TOA location estimators for NLOS environments," in *Proc. IEEE Vehicular Technology Conf. (VTC) Fall*, Vancouver, BC, Sept. 2002, vol. 2, pp. 1178–1181.

[44] S. Al-Jazzar, J. Caffery, Jr., and H.R. You, "A scattering model based approach to NLOS mitigation in TOA location systems," in *Proc. IEEE Vehicular Technology Conf. (VTC) Spring*, Birmingham, AL, May 2002, pp. 861–865.

[45] B.L. Le, K. Ahmed, and H. Tsuji, "Mobile location estimator with NLOS mitigation using Kalman filtering," in *Proc. IEEE Wireless Communications and Networking (WCNC'03)*, New Orleans, LA, Mar. 2003, vol. 3, pp. 1969–1973.

[46] B. Denis, J. Keignart, and N. Daniele, "Impact of NLOS propagation upon ranging precision in UWB systems," in *Proc. IEEE Conf. Ultra Wideband Systems and Technologies (UWBST'03)*, Reston, VA, Nov. 2003, pp. 379–383.

[47] V. Lottici, A. D'Andrea, and U. Mengali, "Channel estimation for ultra-wideband communications," *IEEE J. Select. Areas Commun.*, vol. 20, no. 12, pp. 1638–1645, Dec. 2002.

[48] H. Lee, B. Han, Y. Shin, and S. Im, "Multipath characteristics of impulse radio channels," in *Proc. Vehicular Technology Conf.*, Tokyo, Japan, Spring 2000, pp. 2487–2491.

[49] IEEE 802.15 WPAN High Rate Alternative PHY Task Group 3a (TG3a), Dec. 2002 [Online]. Available: http://www.ieee802.org/15/pub/TG3a.html

[50] M.Z. Win and R.A. Scholtz, "Ultra wide bandwidth time-hopping spread-spectrum impulse radio for wireless multiple access communications," *IEEE Trans. Commun.*, vol. 48, pp. 679–691, 2000.

[51] C.J. Le Martret and G.B. Giannakis, "All-digital impulse radio for wireless cellular systems," *IEEE Trans. Commun.*, vol. 50, no. 9, pp. 1440–1450, Sept. 2002.

[52] A.R. Forouzan, M. Nasiri-Kenari, and J.A. Salehi, "Performance analysis of ultra-wideband time-hopping spread spectrum multiple-access systems: Uncoded and coded systems," *IEEE Trans. Wireless Commun.*, vol. 1, no. 4, pp. 671–681, Oct. 2002.

[53] M. Moeneclaey, "A fundamental lower bound on the performance of practical joint carrier and bit synchronizers," *IEEE Trans. Commun.*, vol. COM-32, no. 9, Sept. 1984, pp. 1007–1012.

[54] A. D'Andrea, U. Mengali, and R. Reggiannini, "The modified Cramer-Rao bound and its application to synchronization problems," *IEEE Trans. Commun.*, vol. 42, pp. 1391–1399, Feb.–Apr. 1994.

[55] D. Cassioli, M.Z. Win, and A.F. Molisch, "The ultra-wide bandwidth indoor channel: From statistical model to simulations," *IEEE J. Select. Areas Commun.*, vol. 20, no. 6, pp. 1247–1257, Aug. 2002.

[56] A.F. Molisch, J.R. Foerster, and M. Pendergrass, "Channel models for ultrawideband personal area networks," *IEEE Wireless Commun.*, vol. 10, no. 6, pp. 14–21, Dec. 2003.

[57] M.Z. Win and R.A. Scholtz, "On the energy capture of ultrawide bandwidth signals in dense multipath environments," *IEEE Commun. Letters*, vol. 2, pp. 245–247, Sept. 1998.

[58] R.C. Qiu, "A study of the ultra-wideband wireless propagation channel and optimum UWB receiver design," *IEEE J. Select. Areas Commun.*, vol. 20, no. 9, pp. 1628–1637, Dec. 2002.

[59] Z. Wang and X. Yang, "Ultra wide-band communications with blind channel estimation based on first-order statistics," in *Proc. IEEE Int. Conf. Acoustics, Speech, and Signal Processing (ICASSP'04)*, May 17–21, 2004, vol. 4, pp. 529–532.

[60] R. Hoctor and H. Tomlinson, "Delay-hopped transmitted-reference RF communications," in *Proc. IEEE Conf. UWB Syst. and Tech.*, Baltimore, MD, May 2002, pp. 265–269.

[61] J. Borras, P. Hatrack, and N.B. Mandayam, "Decision theoretic framework for NLOS identification," in *Proc. IEEE Vehicular Technology Conf. (VTC'98 Spring)*, Ottowa, Canada, May 18–21, 1998, vol. 2, pp. 1583–1587.

[62] S. Gezici, H. Kobayashi, and H.V. Poor, "Non-parametric non-line-of-sight identification," in *Proc. IEEE 58th Vehicular Technology Conf. (VTC 2003 Fall)*, Orlando, FL, Oct. 6–9, 2003, vol. 4, pp. 2544–2548.

[63] S. Venkatraman and J. Caffery, "A statistical approach to non-line-of-sight BS identification," in *Proc. IEEE 5th Int. Symp. Wireless Personal Multimedia Communications (WPMC 2002)*, Honolulu, Hawaii, Oct. 2002, vol. 1, pp. 296–300.

[64] S. Gezici, H. Kobayashi, H.V. Poor, and A.F. Molisch, "Performance evaluation of impulse radio UWB systems with pulse-based polarity randomization," *IEEE Trans. Signal Processing*, to be published.

[65] H.L. Van Trees, *Detection, Estimation and Modulation Theory, Part 1*. New York: Wiley, 1998.

[66] A.E. Leu and B.L. Mark, "Modeling and analysis of fast handoff algorithms for micro-cellular networks," in *Proc. IEEE/ACM MASCOTS 2002*, Fort Worth, TX, Oct. 2002, pp. 321–328.

[67] A.E. Leu and B.L. Mark, "A discrete-time approach to analyze hard handoff performance," *IEEE Trans. Wireless Comm.,* vol. 3, no. 5, pp. 1721–1733, Sept. 2004.

[68] N. Patwari, A.O. Hero, M. Perkins, N.S. Correal, and R.J. O'Dea, "Relative location estimation in wireless sensor networks," *IEEE Trans. Signal Processing*, vol. 51, pp. 2137–2148, Aug. 2003.

[69] A.F. Molisch, "Status of channel modeling," IEEE P802.15-04-0346-00-004a/r0, IEEE P802.15 Study Group 4a for Wireless Personal Area Networks (WPANs), July 2004 [Online]. Available: *http://802wirelessworld.com*   SP